1-8-2015

Monomials and Basin Cylinders for Network Dynamics

Daniel Austin
Oregon Health & Science University

Ian H. Dinwoodie
Portland State University

Citation Details

Austin, D., & Dinwoodie, I. H. (2015). Monomials and Basin Cylinders for Network Dynamics. SIAM Journal on Applied Dynamical Systems, 14(1), 25-42.

SIAM J. Applied Dynamical Systems
Vol. 14, No. 1, pp. 25–42

Monomials and Basin Cylinders for Network Dynamics*

Daniel Austin† and Ian H. Dinwoodie‡

Abstract. We describe methods to identify cylinder sets inside a basin of attraction for Boolean dynamics of biological networks. Such sets are used for designing regulatory interventions that make the system evolve toward a chosen attractor, for example, initiating apoptosis in a cancer cell. We describe two algebraic methods for identifying cylinders inside a basin of attraction, one based on the Groebner fan that finds monomials that define cylinders, and the other on primary decomposition. Both methods are applied to current examples of gene networks.

Key words. apoptosis, asynchronous network, basin of attraction, Boolean network, Groebner basis, Groebner fan, prime decomposition

AMS subject classifications. 37N25, 13P25, 13P10

DOI. 10.1137/140975929

1. Introduction.

Boolean networks are conceptual tools for understanding dynamics of biological systems such as signalling and regulatory networks. A Boolean network is a discrete dynamical system with binary state space which evolves over time using a transition map F. Biological modeling with Boolean networks goes back at least to Thomas [39], and they continue to be widely used [3], [20], [27], [34], [35], [36], [37].

Eventually the system will terminate in an attracting set, which is either a fixed point or a finite cycle. The attracting set may have practical importance, such as a state of "apoptosis" in which a cancer cell is eliminated [36]. A recent use of the Boolean model is to help identify therapeutic interventions [23], [24], [31], [32]. By this is meant a configuration or assignment of values to a subset of nodes which guarantees that the network will terminate in a specific desirable attractor. As described in [32], the goal is to find component perturbations or node assignments that lead to cancer cell death. These components could be further studied as candidates for therapeutic intervention.

To motivate the results and introduce terminology, consider a simple fictional network for illustration. The network is an oversimplified version of the $p53$ tumor suppressor gene pathway. The network has two nodes, Apoptosis and $p53$ numbered 1 and 2, taking values 0 and 1 for off/on. The dynamics will be defined as $p53$ turning on Apoptosis for tumor suppression, pictured in Figure 1. This can be written logically as $\text{Apoptosis}^{t+1} = p53^t$, and $p53^{t+1} = p53^t$ with discrete time index t. This notation defines a fixed transition map from any state (x_1, x_2) to the next state of the system, where, for example, (0,1) transitions to (1,1).

*Received by the editors July 7, 2014; accepted for publication (in revised form) by R. Albert October 31, 2014; published electronically January 8, 2015.
http://www.siam.org/journals/siads/14-1/97592.html
†Department of Neurology, Oregon Health & Science University, Portland, OR 97239 (austidan@ohsu.edu). The work of this author was supported by NIH R01AG024059, P30 AG024978, and P30 AG008017.
‡Fariborz Maseeh Department of Mathematics and Statistics, Portland State University, Portland, OR 97201 (ihd@pdx.edu).

Figure 1. *Example: Node* 2 *activates node* 1.

The dynamical system has two steady states, (0,0) and (1,1). The desirable steady state is (1,1), where Apoptosis is on, and our question is which starting states in the system will terminate in this configuration. It is easy to see that states (0,1) and (1,1) both lead to (1,1). These two points together make a *cylinder*, meaning that a subset of coordinates are fixed at particular values and the other coordinates are free. This can be written as $C = \{(x_1, x_2) : x_2 = 1\}$. Now one can say that any network configuration with $x_2 = 1$ will terminate with $x_1 = 1$, the desirable attractor, and setting $x_2 = 1$ would be called a component perturbation and node 2 would be a therapeutic target.

A basin of attraction is the set of states which eventually lead to a particular attractor or steady state. This example shows the importance of identifying subsets of a basin of attraction defined by restricting a few coordinates—set only those coordinates to the right values, and the state will reach the attractor regardless of the other coordinate values. The restricted coordinates are the targets for an intervention, and they also define a cylinder subset of the basin of attraction. Mathematically, the question becomes how to find cylinders inside a basin of attraction. Theorems 2.1 and 2.2 give two ways to do this.

The mathematical tools come from commutative algebra and algebraic geometry, where sets of points can be represented as roots of multivariate polynomials to take advantage of computational algorithms implemented in algebra software. The main mathematical ideas are to represent a basin of attraction with its ideal—the polynomials that vanish on all points on the basin—and to use established connections between the geometry of the basin and its algebra. Theorem 2.1 finds equations that must all be satisfied for a state *not* to be in the basin of attraction, then contradicts the simple ones (monomials) to guarantee inclusion. In our example, the basin is described algebraically by the equation $x_2 = 1$, which is written as $x_2 - 1 = 0$ or simply $x_2 - 1$ in algebraic geometry. Then the procedure finds the monomial x_2 as the equation for the complement of the basin of attraction using the colon ideal (interpreted as $x_2 = 0$), and contradicting that equation with $x_2 = 1$ gives a cylinder condition for inclusion in the basin. This method is more interesting when the basin is not defined by a single equation. In contrast, Theorem 2.2 is a direct analysis of the equations defining the basin using the classical prime decomposition which finds simple subsets of the basin by identifying corresponding prime components in the algebra.

Based on our examples, Theorem 2.2 is the more powerful method, but there may be examples where Theorem 2.1 is more useful.

Computations can be done in any of the algebra software systems Cocoa [1], Macaulay2 [15], or Singular [9]; ours were done in Singular. Theoretical complexity results on the underlying algebra calculations [12] essential to computational algebra do not promise scalability, but the methods seem to work well on real examples from the biology literature, for which worst-possible-case complexity bounds are too pessimistic. Other computational tools for studying basins are available, including BoolNet [28] and DDLab [40]. Simulation has been a common tool for understanding basins of attraction. However, for finding states that

lead to a certain attractor it may be necessary to perturb many nodes simultaneously in the network, as a single node value will generally not determine the final state. In the T cell network of Example 3.3, it is necessary to set the values of three nodes to guarantee apoptosis. The algebraic approach of this paper will find multidimensional interventions, and it provides geometrical insight useful for applications.

Variations on pure deterministic dynamics such as asynchronous updates [6] are of interest in biology, and those are also possible here (see Example 3.3); one need only represent the basin algebraically as a variety for an ideal $I_B \subset \mathbb{C}[\mathbf{s}]$ (see [10] for an algorithm in the case of a steady-state attractor). Generalizations to more than two states are also possible.

2. Results. For Boolean networks, define the binary state space $H = \{0,1\}^d$ and let $F = (F_1, \ldots, F_d) : H \to H$ be a transition map. For an attracting set $A \subset H$ (the limiting set of any initial state and either a fixed point or limit cycle), define its basin of attraction B as

$$B := \cup_{k=1}^{\infty} \{\mathbf{x} \in H : F^k(\mathbf{x}) \in A\}. \tag{2.1}$$

The results of this section are about finding simple subsets C of B. Note that if $C \subset B$, then any state in C will converge to the attractor A that defines B. Our primary focus will be on subsets C defined by fixing some coordinates and leaving others free,

$$C = \{\mathbf{x} \in H : x_{i_1} = a_1, \ldots, x_{i_c} = a_c\},$$

which we call *cylinder sets*. Then if $C \subset B$, setting the values of coordinates $i_1, \ldots, i_c$ to $a_1, \ldots, a_c$ on any state $\mathbf{x}$ ensures membership in B and convergence to the attractor A.

Variations on the basin B above for deterministic or synchronous dynamics have been introduced when randomized versions of F are of interest. In particular, if one coordinate map of F is chosen randomly at each time step instead of all coordinates applied simultaneously, then the *exclusive basin of attraction* is the set of points that reach A with probability 1, generally a proper subset of B (see [6], [32] for definitions and examples). All of our results also apply to exclusive basins with asynchronous updates as in Example 3.3. However, the methods of this paper require that the basin be represented by its ideal (the polynomials that vanish on the basin). The method of [10] will compute the ideal for the exclusive basin for a steady state with asynchronous dynamics, and the method of [11] will compute the ideal for the standard basin for an attracting cycle with traditional synchronous dynamics. At this time a method has not been clearly articulated to find the exclusive basin ideal with asynchronous updates for an attracting cycle. With a complete enumeration of states in any type of basin, the ideal can be constructed in a straightforward way as in [2], and working purely algebraically (as in [10]) a more efficient algorithm can surely be formulated.

Let $\mathbb{C}[\mathbf{s}] = \mathbb{C}[s_1, \ldots, s_d]$ be the ring of polynomials with indeterminates $s_1, \ldots, s_d$ and let $\mathbb{C}[\mathbf{s}, \mathbf{t}]$ be the ring of polynomials in $s_1, \ldots, s_d, t_1, \ldots, t_d$. We are using indeterminates $\mathbf{s}$ and $\mathbf{t}$ to distinguish them from states $\mathbf{x}$ and $\mathbf{y}$ in H. The ideal I_B is the set of polynomials f in $\mathbb{C}[\mathbf{s}]$ which vanish at all points in B:

$$I_B := \{f : f(\mathbf{x}) = 0, \mathbf{x} \in B\}. \tag{2.2}$$

The domain H has ideal

$$I_{01} = \langle s_1^2 - s_1, \ldots, s_d^2 - s_d \rangle \subset \mathbb{C}[\mathbf{s}].$$

Note that $B \subset H$ so $I_{01} \subset I_B$, the inclusions are reversed. Each coordinate map $F_j : H \to \{0,1\}$ can always be written as a polynomial $p_j \in \mathbb{C}[\mathbf{s}]$. An update s_1 `or` s_2 is written as a polynomial in the form $s_1 + s_2 - s_1 \cdot s_2$, and s_1 `and` s_2 is written as $s_1 \cdot s_2$.

Computational methods and algorithms for multivariate polynomials are built on the notion of Groebner basis. The algebraic algorithms are available in many software packages, and their use does not require that one be a specialist. For the methods of this paper, a unifying interface to the tools would be useful in the same way as a tool for solving differential equations.

Here we give a general overview of the basic notions of computational algebra. A Groebner basis is a particular way to write a generating set of polynomials for an ideal that depends on a special total ordering of monomials called a *term order*. Standard term orders are lexicographic, graded lexicographic, and graded reverse lexicographic. In lexicographic ordering, s_1 is bigger than s_2^2, but in graded lexicographic ordering, s_2^2 is bigger than s_1 in $\mathbb{C}[s_1, s_2]$ because one first looks at the total degree. The Groebner basis has the property that the leading or largest monomials of the polynomials in the Groebner basis set are rich enough to generate all the leading monomials that could be found by looking at combinations of polynomials in the generating set. Formally, suppose polynomials $f_1, \ldots, f_g \in \mathbb{C}[\mathbf{s}]$ generate an ideal $I = \langle f_1, \ldots, f_g \rangle := \{\sum_{j=1}^{g} p_j f_j, p_j \in \mathbb{C}[\mathbf{s}]\}$, and let $LT(f)$ be the largest monomial of a polynomial f for a particular ordering (for example, $LT(s_1^2 - s_1) = s_1^2$). The set $g_1, \ldots, g_b$ in I is a Groebner basis for I if

$$\langle LT(g_1), \ldots, LT(g_b) \rangle = \left\langle LT(f) : f = \sum_{j=1}^{g} p_j f_j \right\rangle.$$

Typically many different term orders will result in the same Groebner basis in a particular example, and the Groebner fan is a geometrical way to classify them in terms of equivalent final basis in that example. For example, the set of points $\{(0,0),(1,1)\}$ has ideal $I = \langle s_1 - s_2, s_2^2 - s_2 \rangle$ (these two polynomials vanish at the two points, and all polynomials that vanish can be written as combinations of the two). The two polynomials $s_1 - s_2, s_2^2 - s_2$ are in fact a Groebner basis in lexicographic order. Now by using the fan we find that all other term orders will give only one other Groebner basis set, namely $s_2 - s_1, s_1^2 - s_1$ which comes from reverse lexicographic order. The Groebner fan is developed rigorously in [38] and is quite technical, but the software Gfan of [18] is user friendly.

Algorithms for finding I_B for both the synchronous and asynchronous case with either steady states or limit cycles are in [10] and [11]. Good references for the algebra are [7] and [21], where clear definitions of the colon ideal, prime or minimal decomposition, radical ideal, and reduced or normal form are given. Much of the algebra is also presented in [30] for related applications in statistics, and the use of algebra for dynamics in biological networks is explained in [22] and [37].

Theorem 2.1. *Suppose a monomial* $\prod_{j=1}^{c} s_{i_j}^{a_j} t_{i_j}^{1-a_j}, a_i \in \{0,1\}$, *is in some reduced Groebner basis for the ideal*

$$I = I_{01} : I_B + \langle s_1 + t_1 - 1, s_2 + t_2 - 1, \ldots, s_d + t_d - 1 \rangle \subset \mathbb{C}[\mathbf{s}, \mathbf{t}].$$

Then the cylinder $C_a = \{\mathbf{x} : x_{i_1} = a_1, \ldots, x_{i_c} = a_c\}$ *belongs to the basin of attraction* B.

Proof. Since H and B are finite sets and therefore varieties, we have that $I_{01} : I_B$ is the ideal for the finite set $H-B \subset \mathbb{C}^d$ [7, p. 193]. Now in $\mathbb{C}[\mathbf{s},\mathbf{t}]$, $I = I_{01} : I_B + \langle s_1+t_1-1, s_2+t_2-1, \ldots, s_d+t_d-1\rangle$ is the ideal for the variety $(H-B)\times\mathbb{C}^d \cap \{x_1+y_1=1,\ldots,x_d+y_d=1\} \subset \mathbb{C}^{2d}$ since it is radical by Seidenberg's lemma [21, p. 250]. Thus a polynomial $f \in I$ will vanish at every point $(\mathbf{x},\mathbf{y}) \in H \times H$ with $\mathbf{x} \in B$ and $\mathbf{y} = 1-\mathbf{x}$. If a polynomial $f \in I$ does not vanish at a point $(\mathbf{x}, 1-\mathbf{x}) \in H \times H$, then $\mathbf{x} \notin H - B$. But if $\mathbf{x} \in H$, this implies that $\mathbf{x} \in B$, the basin of attraction.

Now let $f = \prod_{j=1}^{c} s_{i_j}^{a_j} t_{i_j}^{1-a_j}, a_j \in \{0,1\}$, hypothetically appear as an element of a reduced Groebner basis of I for any term order. The set of points $C_a := \{\mathbf{x} : x_{i_j} = a_j, j = 1,\ldots,c\}$ all satisfy $f(\mathbf{x}, 1-\mathbf{x}) = 1$, showing that $\mathbf{x} \in B$. Thus C_a is a cylinder in B. ∎

To summarize Theorem 2.1 for applications, if a state $\mathbf{x} \in \{0,1\}^d$ is *not* a root of some polynomial in $I_{01} : I_B$, it will belong to B. Thus any monomial $\prod_{j=1}^{c} s_{i_j}^{a_j} t_{i_j}^{1-a_j} \in I_{01} : I_B$ gives the equation for *inclusion* in B:

$$\prod_{j=1}^{c} s_{i_j}^{a_j} t_{i_j}^{1-a_j} = 1,$$

where x_i is a value of s_i, and $1-x_i$ is for t_i. Its solution set $x_{i_j} = a_j$, $j = 1,\ldots,c$, is a cylinder in B. This cylinder is a vanishing configuration in the complement B^c in the terminology of [10]. The way to look at all reduced Groebner bases is with the Groebner fan [38], [13] and software Gfan [18]. So the procedure for applying Theorem 2.1 is to compute I_B in $\mathbb{C}[\mathbf{s}]$ and then inject I_B and I_{01} into the larger ring $\mathbb{C}[\mathbf{s},\mathbf{t}]$, where Gfan can be used to compute all the Groebner bases in various term orders. The number of bases can be quite large, so finding monomials is best done with text search algorithms. This method works on most of the examples in section 3, but Theorem 2.1 has two weaknesses. First, the fan computations can be quite complex, as in Example 3.5, where the Gfan output exceeded 1 gigabyte of file size without terminating. Second, sometimes a monomial for a cylinder strictly inside B may not appear, as in Example 2.1 below.

Example 2.1. Suppose $d = 2$ and $B = \{00, 01\}$, which can be written as $0*$, where $*$ is a wild card placeholder. Then $I_B = \langle s_1, s_2^2 - s_2\rangle$, and the colon ideal $I_{01} : I_B$ for points *not* in B has generating set $\langle s_1 - 1, s_2^2 - s_2\rangle$. We can see the cylinder in B defined by $s_1 - 1 = 1$. Adding the equations $s_1 + t_1 - 1, s_2 + t_2 - 1$ will make it a monomial as $s_1 - 1$ is effectively $-t_1$ for solutions. Using Gfan [18], we see two reduced Groebner bases,

$$G_1 = \{t_2^2 - t_2, t_1, s_2 - 1 + t_2, s_1 - 1\},$$
$$G_2 = \{t_2 - 1 + s_2, t_1, s_2^2 - s_2, s_1 - 1\},$$

and the monomial t_1 appears, corresponding to solution $t_1 = 1 - s_1 = 1$. The monomial form is useful in complicated examples where cylinders are not so easily seen by inspection.

Now, let a different basin $B = \{00, 11\}$. Then one Groebner basis for I in Theorem 2.1 is given by $\{t_1 + t_2 - 1, s_2 + t_2 - 1, s_1 + t_1 - 1, t_2^2 - t_2\}$, and none of the four Groebner bases reveals monomials t_1t_2 or s_1s_2 for the trivial subcylinders 00 and 11, so here Theorem 2.1 is not effective.

Proposition 2.1. *Let B be a basin of attraction and suppose that $I_B = J + I_{01}$ where $J \subset \mathbb{C}[s_{i_1},\ldots,s_{i_c}]$. Then there is a cylinder on coordinates $i_1,\ldots,i_c$ contained in the basin B.*

Proof. Let $\mathbf{x} \in B \subset \{0,1\}^d$ satisfy the equations in I and I_{01}. Consider the cylinder $C = \{\mathbf{y} = (y_1, \ldots, y_d) : y_j = x_j, j = i_1, \ldots, i_c, y_i = 0, 1\}$. These points satisfy the equations in both I and I_{01}; hence they all belong to the variety B defined by I_B. ∎

Proposition 2.1 can be applied by inspection in some examples such as Example 3.1. A way to compute J in $I_B = J + I_{01}$ is to reduce a generating set for I_B by a Groebner basis for I_{01}:

$$I_B = \bar{I}_B + I_{01},$$

where $\bar{I}_B := \langle \bar{f}_i, i = 1, \ldots, b\rangle, I_B = \langle f_i, i = 1, \ldots, b\rangle$, and $\bar{f}$ is the remainder or normal form when f is divided by the Groebner basis for I_{01}. This uses $I_{01} \subset I_B$ which follows from (2.2). Here is a simple example. Suppose that $d = 2$ and $B = \{00, 01\}$ as in Example 2.1. Then $I_B = \langle s_1, s_2^2 - s_2\rangle$, which has the form

$$I_B = \langle s_1\rangle + \langle s_1^2 - s_1, s_2^2 - s_2\rangle$$

since the generators in I_B can be written as sums $fs_1 + g(s_2^2 - s_2)$. This reveals the cylinder $x_1 = 0$, the roots of s_1 in H.

Finally we treat the general case where a basin of attraction is a union of smaller cylinders.

Theorem 2.2. *Let $I_B = \bar{I} + I_{01}$ and let $\sqrt{\bar{I}}$ have minimal decomposition $\cap_k P_k$, where P_k is prime and not contained in any other P_j. Suppose $P_i \subset \mathbb{C}[s_{i_1}, \ldots, s_{i_c}]$ is in an elimination ideal. Then any binary solution $\mathbf{a} = (a_{i_1}, \ldots, a_{i_c})$ to the equations in P_i defines a cylinder set $C_a = \{\mathbf{x} : x_j = a_j, j = i_1, \ldots, i_c, x_i = 0, 1\} \subset H$ of size 2^{d-c} contained in the basin B. Furthermore, if $\bar{I}$ has a generating set that is reduced with respect to a Groebner basis for I_{01}, then every cylinder $C_a \subset B$ will arise in this way.*

Proof. Let $\mathbf{a} = (a_{i_1}, \ldots, a_{i_c}) \in \{0,1\}^c$ solve all the equations in P_i, meaning $\mathbf{a}$ is a root for all the generators in indeterminates $s_{i_1}, \ldots, s_{i_c}$. Set $C_a = \{\mathbf{x} : x_j = a_j, j = i_1, \ldots, i_c, x_i = 0, 1\}$. These points satisfy the equations in both $\cap_k P_k$ and I_{01}; hence they all belong to the variety of $\sqrt{\bar{I}} + I_{01}$. This means they belong to the variety V of $\bar{I}$, since it is the same as the variety of $\sqrt{\bar{I}}$, and they also have binary coordinates $x_i = 0, 1$. But since $I_B = \bar{I} + I_{01}$, this shows that points in C_a satisfy all the equations in I_B, and hence they belong to the basin B.

Now, suppose $C_a \subset B$ with $C_a = \{\mathbf{x} : x_j = a_j, j = i_1, \ldots, i_c, x_i = 0, 1\}$ being any cylinder in B. Since $C_a \subset B$, their ideals have the opposite inclusion:

$$I_a + I_{01} \supset \bar{I} + I_{01},$$

where $I_a = \langle s_{i_1} - a_{i_1}, \ldots, s_{i_c} - a_{i_c}\rangle$ is prime. Under the assumption that $\bar{I}$ has generators reduced with respect to I_{01}, this implies that $I_a \supset \bar{I}$. Indeed, let $f \in \bar{I}$ be a generator with $f = \bar{f}$; that is, f is reduced for I_{01}. Recall that $\bar{f}$ is notation for the normal or reduced form of f, computed as the remainder when f is divided by a Groebner basis for I_{01}, and no term of $f = \bar{f}$ is divisible by any of the lead terms s_k^2, $k = 1, \ldots, d$ [7, p. 81]. Since $f \in I_a + I_{01}$, f reduces to zero when divided by a Groebner basis for $I_a + I_{01}$, and $\{s_1^2 - s_1, \ldots, s_d^2 - s_d, s_{i_1} - a_{i_1}, \ldots, s_{i_c} - a_{i_c}\}$ is a Groebner basis in lexicographic order. Now in the division algorithm, none of the quadratic terms $s_i^2 - s_i$ will be involved since no term of f is divisible by any of them; hence the representation by the division algorithm will give

$$f = \sum_k q_k(s_{i_k} - a_{i_k}) + \sum_k 0 \cdot (s_k^2 - s_k),$$

showing that $f \in I_a$. Now with $\bar{I} \subset I_a$ we also have $\sqrt{\bar{I}} \subset I_a$ as I_a is radical. With minimal decomposition $\cap_k P_k = \sqrt{\bar{I}} \subset I_a$ into prime ideals P_k, it is elementary that one of the primes belongs to the prime I_a:

$$P_i \subset I_a.$$

Then, any point $\mathbf{x}$ with $x_{i_1} = a_{i_1}, \ldots, x_{i_c} = a_{i_c}$ satisfies the equations in P_i because such a point satisfies the equations in I_a. Thus we have shown that the cylinder C_a can be described as coming from a particular solution $\mathbf{a}$ to equations in an ideal P_i in the prime decomposition of $\sqrt{\bar{I}}$, where P_i is generated by polynomials using a subset of indeterminates. ∎

Theorem 2.2 gives a computational method for finding subcylinders in B: reduce generators of I_B with a Groebner basis of I_{01}, then find a prime decomposition of its radical and look for components that use a subset of indeterminates. This powerful method is used in Example 3.5 below based on a network in Handorf and Klipp [16]. To clarify the second part of the theorem, suppose that a basin B in $d = 3$ is a cylinder 0**. Then its ideal I_B can be written as

$$I_B = \langle s_1 \rangle + I_{01},$$

and we see that $P_1 = \langle s_1 \rangle \subset \mathbb{C}[s_1]$ is the only prime component. Then we can use $\mathbf{a} = (0)$ for the complete basin cylinder 0**, $\mathbf{a} = (0, 0)$ for subcylinder 00*, or $\mathbf{a} = (0, 0, 0)$ for trivial cylinder 000—in all cases $\mathbf{a}$ is a root of the equations in P_1, but there is not a unique root. Also observe that reducing a generating set for I_B may not immediately produce a radical $\bar{I}$. For example, in $d = 2$, I_B may be written as $\langle s_1 s_2, s_1^2 - s_1 s_2, s_1^2 - s_1, s_2^2 - s_2 \rangle$; then reducing I_B gives generators $\bar{I} = \langle s_1 s_2, s_1 s_2 - s_1 \rangle$, which is not a radical ideal, and finally $\sqrt{\bar{I}} = \langle s_1 \rangle$.

3. Examples. We apply the methods to five examples with 4–14 nodes. The method of primary decomposition of Theorem 2.2 works well on all of the examples. However, the method based on the Groebner fan of Theorem 2.1 does not terminate after hours of computing time for one attractor in the most complex example, Example 3.5, where the basin is a union of 28 small cylinders.

The state graphs were done with BoolNet [28], where the vertex labels in binary form always appear upwards and to the right of the corresponding vertex, up a short northeast line segment and not always closest to the corresponding vertex. The graphs are all for synchronous dynamics, and the colors or shading of the graphs differentiate basins based on synchronous dynamics. In Example 3.3 we find cylinder subsets of the exclusive basin of attraction for asynchronous dynamics, but its state space graph in Figure 7 is for the synchronous dynamics as given by BoolNet for consistency. The exclusive basin of attraction is strictly smaller than the standard basin in this example, and the asynchronous state space is graphed in [32]. Both Theorems 2.1 and 2.2 can be applied to any type of basin B if its ideal I_B is given or found.

Example 3.1. Giacomantonio and Goodhill [14] present a Boolean network for gene expression in cerebral cortex development shown in Figure 2. The genes involved are labelled *Fgf*8, *Emx*2, *Pax*6, *Coup-tfi*, and *Sp*8, the network is found by using a literature of interactions to define a search space of 2^{24} functions or networks, and selection is made from this space using experimental expression data. The dynamics in logic without the time index and

algebra (with logical expressions using ! for "not" and & for "and") are

$$\begin{aligned} Fgf8 &= Fgf8 \ \&\ !Emx2 \ \&\ Sp8, & p_1 &= s_1 \cdot (1-s_2) \cdot s_5, \\ Emx2 &= !Fgf8 \ \&\ !Pax5 \ \&\ Coup\text{-}tfi \ \&\ !Sp8, & p_2 &= (1-s_1) \cdot (1-s_3) \cdot s_4 \cdot (1-s_5), \\ Pax6 &= !Emx2 \ \&\ !Coup\text{-}tfi \ \&\ Sp8, & p_3 &= (1-s_2) \cdot (1-s_4) \cdot s_5, \\ Coup\text{-}tfi &= !Fgf8 \ \&\ !Sp8, & p_4 &= (1-s_1) \cdot (1-s_5), \\ Sp8 &= Fgf8 \ \&\ !Emx2, & p_5 &= s_1 \cdot (1-s_2). \end{aligned}$$

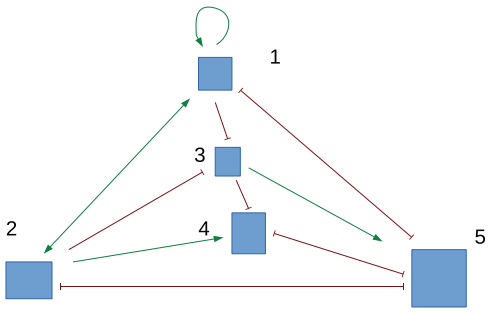

Figure 2. *Example 3.1 network graph for cerebral cortex development.*

The system has two attractors in the form of steady states 01010 and 10101, called *posterior* and *anterior* in [14], pictured in Figure 3. For the first steady state, Theorem 2.2 shows three prime components $P_1 = \langle s_5 \rangle, P_2 = \langle s_2 - 1 \rangle, P_3 = \langle s_1 \rangle$ each defining a cylinder of size 2^4. The basin size is 28, consistent with the counting formula $16 + 16 + 16 - 8 - 8 - 8 + 4$ for a three-way union with intersections of size 2^3 and 2^2. The component P_3 shows that setting $x_1 = 0$ ($Fgf8 = 0$, the roots to the equation s_1) guarantees that the system will evolve toward the posterior steady state 01010; no other components need to be targeted. (Using the Groebner fan of Theorem 2.1 gives monomials t_5, t_1, s_2 which correspond to cylinders $x_5 - 1 = 1, x_1 - 1 = 1, x_2 = 1$ as revealed by the prime decomposition.)

For the anterior fixed point 10101, its basin of size 4 can be found using Proposition 2.1 ($J = \langle s_5 - 1, s_2, s_1 - 1 \rangle$ is found by inspection) or Theorem 2.2, where there is one component P_1 in the prime decomposition $P_1 = \langle s_5 - 1, s_2, s_1 - 1 \rangle$. This gives the cylinder 10**1 as the entire basin (here * is a wild card for that component). Now we see that it is not sufficient to set $x_1 = 1$ ($Fgf8 = 1$) in order to reach the anterior fixed point—one must target three components 1, 2, and 5. (Applying the Groebner fan of Theorem 2.1 reveals 32 Groebner bases with the monomial $s_1 s_5 t_2$ corresponding to cylinder $x_1 = 1, x_5 = 1, x_2 - 1 = 1$.)

In [14] the role of $Fgf8$ in determining the final steady state in this model is discussed. Our analysis shows precisely that $Fgf8$ by itself can be targeted to get the posterior steady-state pattern, but not to get the anterior steady-state pattern.

Example 3.2. Layek, Datta, and Dougherty [23] study a model of tumor suppressor gene $p53$ pathways, where one node dna_dsb serves as an external signal taking fixed unchanging values 0 or 1 and is intended to model DNA damage input. The dynamics on the other nodes

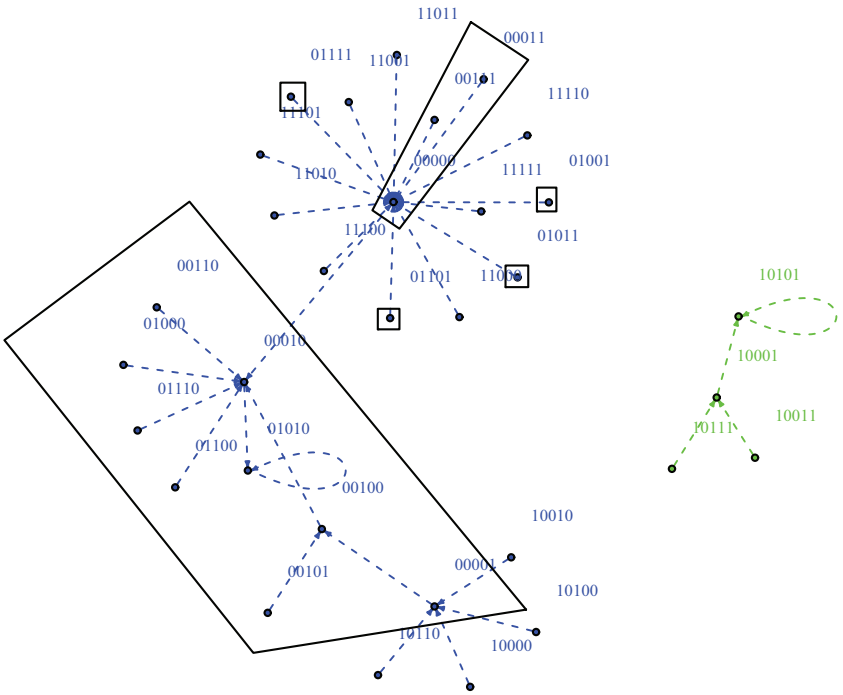

Figure 3. *Example 3.1 state graph for cerebral cortex development (with cylinder $x_1 = 0$ marked in six polygons in blue posterior basin).*

$ATM, p53, Wip1, Mdm2$ represented as indeterminates s_1, s_2, s_3, s_4 are given by

$$\begin{aligned} ATM &= !Wip1 \,\&(ATM \text{ or dna\_dsb}), & p_1 &= (1 - s_3) \cdot (s_1 + \text{dna\_dsb} - s_1 \cdot \text{dna\_dsb}),\\ p53 &= !Mdm2 \,\&\, (ATM \text{ or } Wip1), & p_2 &= (1 - s_4) \cdot (s_1 + s_3 - s_1 \cdot s_3),\\ Wip1 &= p53, & p_3 &= s_2,\\ Mdm2 &= !ATM \,\&\, (p53 \text{ or } Wip1), & p_4 &= (1 - s_1) \cdot (s_2 + s_3 - s_2 \cdot s_3), \end{aligned}$$

and the behavior depends on the value of dna_dsb. The network diagram is in Figure 4.

First consider dna_dsb = 0 for which the system has steady state 0000. The ideal $\bar{I}$ from reducing I_B is just 0, which means the cylinder is the entire state space.

With dna_dsb = 1, there is one limit cycle of size 7:

1000
1100
1110
0110
0111
0011
0001

Here the reduction $\bar{I}$ is again 0, meaning that the basin is the entire domain H. The basins are pictured in Figure 5.

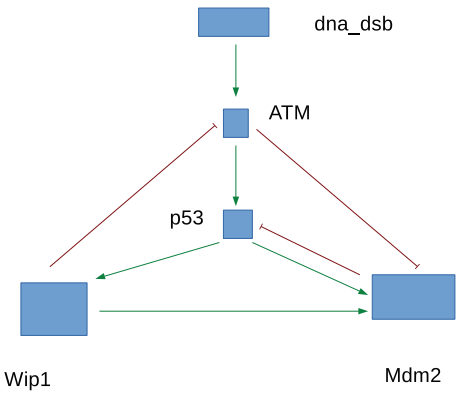

Figure 4. *Example 3.2 network graph for tumor suppressor pathway.*

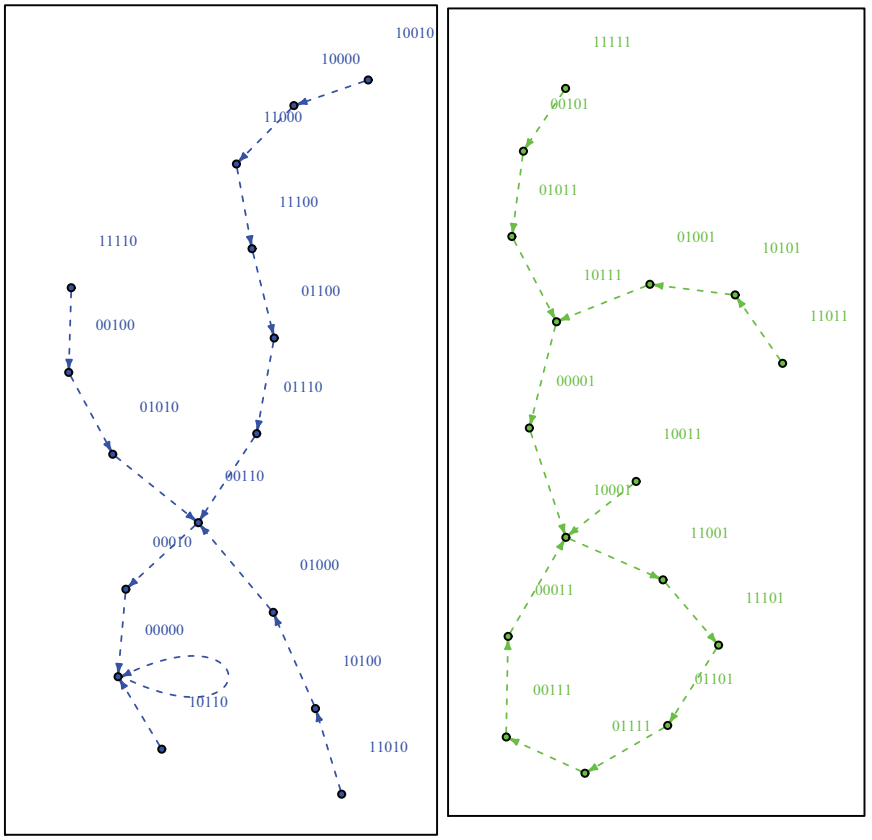

Figure 5. *Example 3.2 state graph for tumor suppressor pathway (with cylinders marked with rectangles containing entire blue dna_dsb = 0 basin and entire green dna_dsb = 1 basin, where dna_dsb is the last coordinate value).*

The conclusion of the analysis is that activation of the genes depends entirely on the value of dna_dsb: when dna_dsb = 0 for no DNA damage, the genes will eventually deactivate to value 0; when dna_dsb = 1 for external stress, the genes will activate in cyclic oscillatory fashion in the order $ATM, p53, Wip1, Mdm2$.

Example 3.3. Here we consider a T cell survival network example from [32], where therapeutic intervention is addressed, and [41]. The goal is to find out what components of the network must be assigned which values in order to terminate with Apoptosis on. Analyzing the (asynchronous) basin of attraction, we see below that we can attain this terminal state by setting S1P = 0, Fas = 1, and Ceramide = 1. These three assignments describe a subset of the basin of attraction of the desired steady state of Apoptosis. The network is shown in Figure 6.

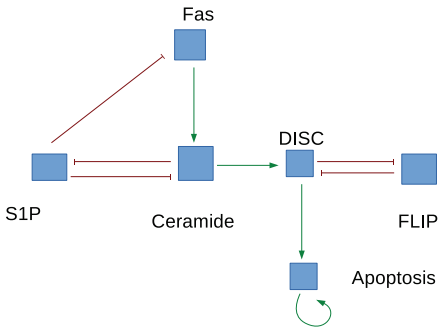

Figure 6. *Example* 3.3 *network graph for T cell survival.*

Table 1 gives the map F on $d = 6$ dimensions taken from Table 1 of [32], where "update" indicates the coordinate function for the next time step, and "not" is written as "!" and "and" as "&" for brevity. This dynamic model has two steady states, a disease steady state D=110000, and a normal steady state N=000001. Dynamics will be asynchronous, meaning that rather than updating all coordinates simultaneously, only one coordinate will be chosen for updating randomly. Methods of [10] will give the exclusive basin of attraction of the normal steady state where apoptosis occurs and eliminates the cancer cell (Apoptosis = 1). The basis is presented in the appendix. By inspection, one sees the polynomials in I_{01} that define the binary states, and four polynomials that use indeterminates 1, 3, 4, and 6. Then, according to Proposition 2.1, coordinates 1, 3, 4, and 6 will be involved in cylinders. Applying Theorem 2.2, we compute $\bar{I} = \langle s_4 s_6 - s_4 - s_6 + 1, s_3 s_6 - s_3 - s_6 + 1, s_1 s_6 - s_1 \rangle$, which is radical. Finally, the primary decomposition has two components $P_1 = \langle s_6 - 1 \rangle, P_2 = \langle s_4 - 1, s_3 - 1, s_1 \rangle$. Thus two cylinders are found: *****1, 0*11**. The second cylinder means the following: if we set coordinates 1, 3, and 4 to values 0, 1, 1, respectively, then the system will evolve toward steady state 000001, regardless of the values of the other coordinates, using asynchronous updates. The union of the two cylinders has size $2^5 + 2^3 - 2^2 = 36$, which is the size of the exclusive basin of attraction.

In the state graph of Figure 7, the blue attractor is the synchronous attractor for the steady state N=000001 for Apoptosis. The asynchronous exclusive basin is smaller, containing only 36 points, and is graphed in [32]. The cylinder 0*11** is inside the smaller exclusive basin.

Example 3.4. Consider an 11-node T cell signalling model relevant to the network of [33].

Table 1
Example 3.3 network maps for T cell survival.

Node	Update	Polynomial
S1P s_1	!(Ceramide or Apoptosis)	$(1-s_4)\cdot(1-s_6)$
FLIP s_2	!(DISC or Apoptosis)	$(1-s_5)\cdot(1-s_6)$
Fas s_3	!(S1P or Apoptosis)	$(1-s_1)\cdot(1-s_6)$
Ceramide s_4	Fas & !(S1P or Apoptosis)	$s_3\cdot(1-s_1)\cdot(1-s_6)$
DISC s_5	(Ceramide or (Fas & !FLIP)) & !Apoptosis	$(1-s_6)\cdot(s_4+(1-s_4)\cdot s_3\cdot(1-s_2))$
Apoptosis s_6	DISC or Apoptosis	$1-(1-s_5)\cdot(1-s_6)$

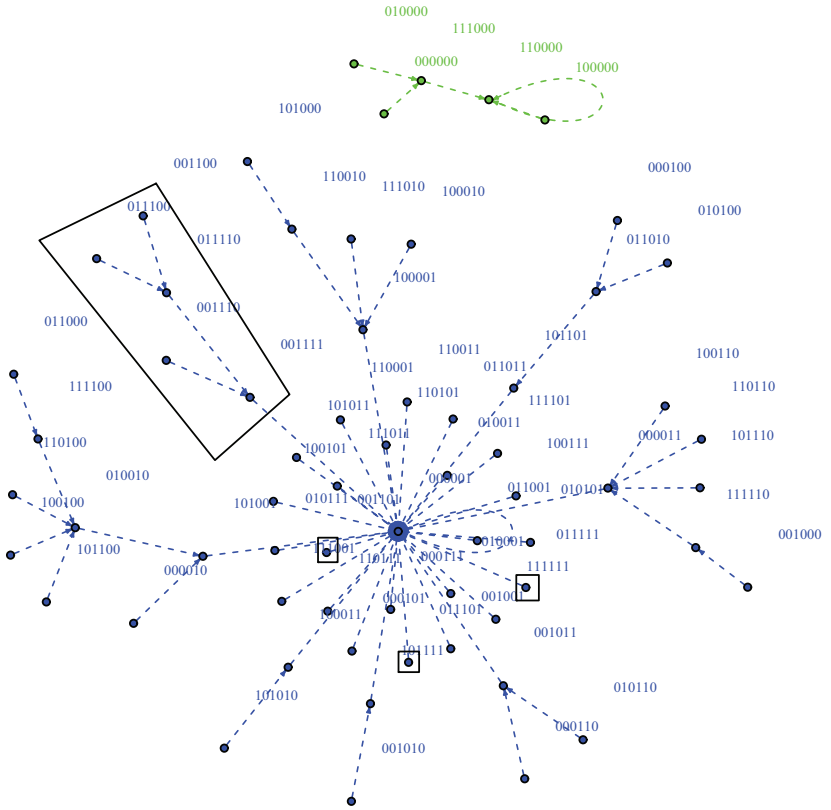

Figure 7. *Example 3.3 synchronous state graph for T cell survival (with cylinder $x_1 = 0, x_3 = 1, x_4 = 1$ marked with four polygons inside the asynchronous exclusive basin which is inside the blue synchronous basin for Apoptosis attractor).*

The dynamics for this model are defined precisely in Table 2. The model has four steady states:

00000000000
11110111111
11011111111
11111111111.

The constant steady states **0** and **1** are immediately seen to have cylinder basins with Proposition 2.1 or Theorem 2.2, the first being **0*0****** and the second **1*1******.

Table 2
Example 3.4 network maps for T cell signalling.

Node	Update	Polynomial
raf s_1	PKA or PKC	$s_8 + s_9 - s_8 \cdot s_9$
mek s_2	raf or PKA or PKC	$1 - (1 - s_1) \cdot (1 - s_8) \cdot (1 - s_9)$
plcg s_3	plcg	s_3
PIP2 s_4	plcg or PIP3	$s_3 + s_5 - s_3 \cdot s_5$
PIP3 s_5	PIP3	s_5
erk s_6	mek or PKA	$s_2 + s_8 - s_2 \cdot s_8$
akts s_7	PIP3 or erk or PKA	$1 - (1 - s_8) \cdot (1 - s_6) \cdot (1 - s_5)$
PKA s_8	PKC	s_9
PKC s_9	plcg or PIP2	$s_3 + s_4 - s_3 \cdot s_4$
P38 s_{10}	PKA or PKC	$s_8 + s_9 - s_8 \cdot s_9$
JNK s_{11}	PKA or PKC	$s_8 + s_9 - s_8 \cdot s_9$

The fan calculations of Theorem 2.1 with Gfan [18] are also fast.

Now for steady state 11110111111, its basin is the cylinder **1*0******. For steady state 11011111111, its basin is cylinder **0*1******. Thus all the basins are simple cylinders determined by nodes 3 and 5, and they can be identified efficiently using any of the three methods.

To apply the analysis, suppose we seek a steady state where erk (node 6) is deactivated at value 0 (this may be related to nonproliferation of T cells, but our example is essentially mathematical). This value of erk is consistent with the one steady state 00000000000, and it *will be reached* if nodes plcg (node 3) and PIP3 (node 5) are deactivated to 0; the values of all other nodes do not matter.

Example 3.5. The 14-node network in Handorf and Klipp [16] involves a Wnt signalling part which is related to aging and Alzheimer's disease [8]. The polynomial dynamics on nodes EGF (1), WNT (2), TCF (3), EGFR (4), X (5), AXIN (6), APC (7), Bcat (8), GSK3 (9), RAS (10), DC (11), cRAF (12), MEK (13), ERK (14) are given by

$$\begin{aligned}
p_1 &= s_1,\\
p_2 &= s_2,\\
p_3 &= s_3,\\
p_4 &= s_1,\\
p_5 &= s_3 \cdot s_8,\\
p_6 &= 1 - s_2,\\
p_7 &= s_7,\\
p_8 &= 1 - s_{11},\\
p_9 &= 1 - s_{14},\\
p_{10} &= s_4 + s_5 - s_4 \cdot s_5,\\
p_{11} &= s_6 \cdot s_7 \cdot s_9,\\
p_{12} &= s_{10} + s_2 - s_{10} \cdot s_2,\\
p_{13} &= s_{12},\\
p_{14} &= s_{13}.
\end{aligned}$$

The system has 51 attractors, including 17 steady states. For steady state 00000101100000 with attracting basin of size 1024, Proposition 2.1 and Theorems 2.1 and 2.2 can all be applied. Its basin B has ideal I_B generated by s_1, s_2, s_3, s_7 as well as the binary equations $s_k^2 - s_k$ on the remaining coordinates, showing immediately a cylinder 000***0*******, where * is a wild card character using Proposition 2.1 ($J = \langle s_1, s_2, s_3, s_7 \rangle$ in Proposition 2.1 by inspection).

To apply Theorem 2.2, note that we get $\bar{I} = \langle s_1, s_2, s_3, s_7 \rangle$ by reducing I_B with I_{01}, and since it is prime no further decomposition is necessary. The elimination ideal P_1 is simply $\langle s_1, s_2, s_3, s_7 \rangle$ as before, giving the cylinder C_a with $\mathbf{a} = (0, 0, 0, 0)$ in coordinates 1, 2, 3, 7.

The Groebner fan of the colon ideal $I_{01} : I_B$ is easily computed and shows 16383 bases. The one monomial $t_1 t_2 t_3 t_7$ appears in 1024 of the bases, confirming the results of the other methods.

For the 8-cycle attractor (60-state basin)

00101111010110
00101111110111
00101111011111
00101110010111
00100111010111
00101111000111
00101111010011
00101111010101

the Groebner fan computations have not been possible, but the decomposition of Theorem 2.2 is fast. The Groebner basis for I_B in graded reverse lexicographic order shows 42 elements. We present them in the appendix. The generators for $I_{01} : I_B$ are more complicated. The prime decomposition of $\sqrt{\bar{I}}$ shows 28 cylinders of sizes 2 and 4, including, for example, 001*1*11011111.

To apply the analysis, suppose the goal is to deactivate ERK (node 14) to 0. There are three attractors with ERK at value 0, including steady state 00000101100000 above and two other steady states. Working within the basin of this steady state, we can attain ERK=0 by setting nodes EGF, WNT, TCF, and APC to 0 (nodes 1, 2, 3, and 7). This is plausible from the wiring diagram in Figure 8. Rules for attaining activation of ERK or oscillatory behavior can also be found, as a complete analysis is possible with Theorem 2.2.

4. Conclusions. We have presented algorithms for analyzing basins of attraction using computational tools of commutative algebra. The methods require the ideal of polynomials for the basin of attraction in a polynomial ring. The algorithms identify cylinder sets within the basin, which can be used for designing interventions that lead to a chosen attractor. Several examples from the current literature on protein and gene interaction models are presented, including an example on inducing apoptosis in a cancer cell, showing the methods to be practical on real examples with up to 15 nodes. Future problems are to extend the methods and algorithms to larger networks of dozens of nodes, such as the $p53$ network in [31] as well as dynamical models on aging and Alzheimer's disease (for example, [5], [8], [17], [25]).

Of particular interest is the Intelligent Systems for Assessing Aging Changes (ISAAC) study [19], a longitudinal aging study conducted by the Oregon Center for Aging Technology (ORCATECH) at Oregon Health & Science University. In this study dozens of variables are

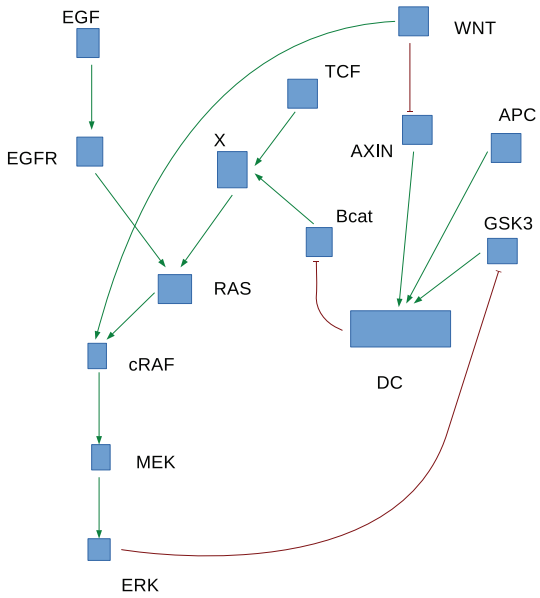

Figure 8. *Example 3.5 network graph for WNT and ERK pathway.*

measured over time, including in-home sensor recordings of walking speed, sleep quality, and mobility [4]. One goal is to understand behavioral dynamics that lead to the undesirable attractor of mild cognitive impairment (MCI), which is associated with increased risk of developing Alzheimer's disease and other dementias [29].

5. Appendix. Equations for Examples 3.3 and 3.5. The following equations define the basin of attraction for the steady state N in Example 3.3:

$$\begin{aligned}
p_1 &= s_6^2 - s_6,\\
p_2 &= s_4 \cdot s_6 - s_4 - s_6 + 1,\\
p_3 &= s_3 \cdot s_6 - s_3 - s_6 + 1,\\
p_4 &= s_1 \cdot s_6 - s_1,\\
p_5 &= s_5^2 - s_5,\\
p_6 &= s_4^2 - s_4,\\
p_7 &= s_3^2 - s_3,\\
p_8 &= s_2^2 - s_2,\\
p_9 &= s_1^2 - s_1.
\end{aligned}$$

The following equations define the basin for the 8-cycle attractor in Example 3.5 (using indeterminate x instead of s):

$x_{14}^2 - x_{14},$

$x_{13}x_{14} - x_{13} - x_{14} + 1,$

$x_{13}^2 - x_{13},$

$$
\begin{aligned}
&x_{12}x_{14} - x_{12} - x_{14} + 1,\\
&x_{12}x_{13} - x_{12} - x_{13} + 1,\\
&x_{12}^2 - x_{12},\\
&x_{11}x_{14} - x_{11},\\
&x_{11}x_{13} - x_{11},\\
&x_{11}x_{12} - x_{11},\\
&x_{11}^2 - x_{11},\\
&x_{10}x_{14} - x_{10} - x_{14} + 1,\\
&x_{10}x_{13} - x_{10} - x_{13} + 1,\\
&x_{10}x_{12} - x_{10} - x_{12} + 1,\\
&x_{10}x_{11} - x_{11},\\
&x_{10}^2 - x_{10},\\
&x_9^2 - x_9,\\
&x_8x_{14} - x_8 - x_{14} + 1,\\
&x_8x_{13} - x_8 - x_{13} + 1,\\
&x_8x_{12} - x_8 - x_{12} + 1,\\
&x_8x_{11} - x_{11},\\
&x_8x_{10} - x_8 - x_{10} + 1,\\
&x_8^2 - x_8,\\
&x_7 - 1,\\
&x_6x_9x_{14} - x_6x_9,\\
&x_6x_9x_{13} - x_6x_9,\\
&x_6x_9x_{12} - x_6x_9,\\
&x_6x_9x_{11},\\
&x_6x_9x_{10} - x_6x_9,\\
&x_6x_8x_9 - x_6x_9,\\
&x_6^2 - x_6,\\
&x_5x_8x_9 - x_5x_8 + x_5x_9x_{10} - x_5x_9x_{11} + x_5x_9x_{12} + x_5x_9x_{13} + x_5x_9x_{14} - 4x_5x_9 - x_5x_{10} + x_5x_{11}\\
&\quad - x_5x_{12} - x_5x_{13} - x_5x_{14} + 4x_5,\\
&x_5x_6x_9 - x_5x_8 - x_5x_{10} + x_5x_{11} - x_5x_{12} - x_5x_{13} - x_5x_{14} + 4x_5,\\
&x_5x_6x_8 + x_5x_6x_{10} - x_5x_6x_{11} + x_5x_6x_{12} + x_5x_6x_{13} + x_5x_6x_{14} - 4x_5x_6 - x_5x_8 - x_5x_{10} + x_5x_{11}\\
&\quad - x_5x_{12} - x_5x_{13} - x_5x_{14} + 4x_5,\\
&x_5^2 - x_5,\\
&x_4x_8x_9 - x_4x_8 + x_4x_9x_{10} - x_4x_9x_{11} + x_4x_9x_{12} + x_4x_9x_{13} + x_4x_9x_{14} - 4x_4x_9 - x_4x_{10} + x_4x_{11}\\
&\quad - x_4x_{12} - x_4x_{13} - x_4x_{14} + 4x_4,
\end{aligned}
$$

$x_4x_6x_9 - x_4x_8 - x_4x_{10} + x_4x_{11} - x_4x_{12} - x_4x_{13} - x_4x_{14} + 4x_4,$

$x_4x_6x_8 + x_4x_6x_{10} - x_4x_6x_{11} + x_4x_6x_{12} + x_4x_6x_{13} + x_4x_6x_{14} - 4x_4x_6 - x_4x_8 - x_4x_{10} + x_4x_{11}$
$- x_4x_{12} - x_4x_{13} - x_4x_{14} + 4x_4,$

$x_4x_5 - x_4 - x_5 + x_6x_9 - x_8 - x_{10} + x_{11} - x_{12} - x_{13} - x_{14} + 5,$

$x_4^2 - x_4,$

$x_3 - 1,$

$x_2,$

$x_1.$

REFERENCES

[1] J. Abbott and A. M. Bigatti, *CoCoALib: A C++ Library for Doing Computations in Commutative Algebra*, http://cocoa.dima.unige.it/cocoalib (2014).

[2] J. Abbott, A. Bigatti, M. Kreuzer, and L. Robbiano, *Computing ideals of points*, J. Symbolic Comput., 30 (2000), pp. 341–356.

[3] R. Albert and H. G. Othmer, *The topology of the regulatory interactions predicts the expression pattern of the segment polarity genes in Drosophila melanogaster*, J. Theoret. Biol., 223 (2003), pp. 1–18.

[4] D. Austin, R. M. Cross, T. Hayes, and J. Kaye, *Regularity and predictability of human mobility in personal space*, PLoS One, 9 (2014), e90256.

[5] F. Caraci, S. Spampinato, M. A. Sortino, P. Bosco, G. Battaglia, V. Bruno, F. Drago, F. Nicoletti, and A. Copani, *Dysfunction of TGF-β1 signaling in Alzheimer's disease: Perspectives for neuroprotection*, Cell Tissue Res., 34 (2012), pp. 291–301.

[6] M. Chaves, R. Albert, and E. D. Sontag, *Robustness and fragility of Boolean models for genetic regulatory networks*, J. Theoret. Biol., 235 (2005), pp. 431–449.

[7] D. Cox, J. Little, and D. O'Shea, *Ideals, Varieties, and Algorithms*, 2nd ed., Springer, New York, 1997.

[8] G. V. De Ferrari and N. C. Inestrosa, *Wnt signaling function in Alzheimer's disease*, Brain Res. Rev., 33 (2000), pp. 1–12.

[9] W. Decker, G.-M. Greuel, G. Pfister, and H. Schönemann, Singular 3-1-6—*A Computer Algebra System for Polynomial Computations*, http://www.singular.uni-kl.de (2012).

[10] I. H. Dinwoodie, *Vanishing configurations in network dynamics with asynchronous updates*, Proc. Amer. Math. Soc., 142 (2014), pp. 2991–3002.

[11] I. H. Dinwoodie and K. Pandya, *Exact tests for singular network data*, Ann. Inst. Statist. Math., to appear.

[12] J. C. Faugère, M. Safey El Din, and T. Verron, *On the complexity of computing Groebner bases for quasi-homogeneous systems*, in Proceedings of the 38th International Symposium on Symbolic and Algebraic Computation (ISSAC '13), Boston, MA, ACM, New York, 2013, pp. 189–196.

[13] K. Fukuda, A. N. Jensen, and R. R. Thomas, *Computing Groebner fans*, Math. Comp., 76 (2008), pp. 2189–2212.

[14] C. E. Giacomantonio and G. J. Goodhill, *A Boolean model of the gene regulatory network underlying mammalian cortical area development*, PLoS Comput. Biol., 6 (2010), e1000936.

[15] D. R. Grayson and M. E. Stillman, *Macaulay2, a Software System for Research in Algebraic Geometry*, http://www.math.uiuc.edu/Macaulay2/ (2014).

[16] T. Handorf and E. Klipp, *Modeling mechanistic biological networks: An advanced Boolean approach*, Bioinformatics, 28 (2012), pp. 557-563.

[17] M. Hermes, G. Eichoff, and O. Garaschuk, *Intracellular calcium signalling in Alzheimer's disease*, J. Cell. Mol. Med., 14 (2009), pp. 30–41.

[18] A. N. Jensen, *Gfan, a Software System for Gröbner Fans and Tropical Varieties*, http://home.imf.au.dk/jensen/software/gfan/gfan.html (2011).

[19] J. A. Kaye, S. A. Maxwell, N. Mattek, T. L. Hayes, H. Dodge, M. Pavel, H. B. Jimison, K. Wild, L. Boise, and T. A. Zitzelberger, *Intelligent systems for assessing aging changes: Home-based, unobtrusive, and continuous assessment of aging*, J. Gerontol. B Psychol. Sci. Soc. Sci., 66B (2011), pp. i180–i190.
[20] S. Klamt, J. Saez-Rodriquez, J. A. Lindquist, L. Simeoni, and E. D. Gilles, *A methodology for the structural and functional analysis of signaling and regulatory networks*, BMC Bioinformatics, 7 (2006), pp. 1471–2105.
[21] M. Kreuzer and L. Robbiano, *Computational Commutative Algebra* I, Springer, New York, 2000.
[22] R. Laubenbacher and B. Sturmfels, *Computer algebra in systems biology*, Amer. Math. Monthly, 116 (2009), pp. 882–891.
[23] R. K. Layek, A. Datta, and E. R. Dougherty, *From biological pathways to regulatory networks*, Mol. BioSyst., 7 (2011), pp. 843–851.
[24] R. K. Layek, A. Datta, M. Bittner, and E. R. Dougherty, *Cancer therapy design based on pathway logic*, Bioinformatics, 27 (2011), pp. 548–555.
[25] T. Lu, L. Aron, J. Zullo, Y. Pan, H. Kim, Y. Chen, T.-H. Yang, et al., *REST and stress resistance in ageing and Alzheimer's disease*, Nature, 507 (2014), pp. 448–454.
[26] L. Mendoza, *A network model for the control of the differentiation process in Th cells*, BioSystems, 84 (2006), pp. 101–114.
[27] M. K. Morris, J. Saez-Rodriguez, P. K. Sorger, and D. A. Lauffenburger, *Logic-based models for the analysis of cell signaling networks*, Biochemistry, 49 (2010), pp. 3216–3224.
[28] C. Müssel, M. Hopfensitz, and H. A. Kestler, *BoolNet—an R package for generation, reconstruction and analysis of Boolean networks*, Bioinformatics, 26 (2010), pp. 1378–1380.
[29] R. C. Petersen, *Mild cognitive impairment as a diagnostic entity*, J. Internal Med., 256 (2004), pp. 183–194.
[30] G. Pistone, E. Riccomagno, and H. P. Wynn, *Algebraic Statistics. Computational Commutative Algebra in Statistics*, Chapman & Hall/CRC Press, Boca Raton, FL, 2000.
[31] R. Poltz and M. Naumann, *Dynamics of p53 and NF-κB regulation in response to DNA damage and identification of target proteins suitable for therapeutic intervention*, BMC Syst. Biol., 6 (2012), 125.
[32] A. Saadatpour, R.-S. Wang, A. Liao, X. Liu, T. P. Loughran, I. Albert, and R. Albert, *Dynamical and structural analysis of a T cell survival network identifies novel candidate therapeutic targets for large granula lymphocyte leukemia*, PLoS Comput. Biol., 7 (2011), e1002267.
[33] K. Sachs, O. Perez, D. Pe'er, D. A. Lauffenburger, and G. P. Nolan, *Causal protein-signaling networks derived from multiparameter single-cell data*, Science, 308 (2005), pp. 523–529.
[34] J. Saez-Rodriquez, L. G. Alexopoulos, M. Zhang, M. Morris, D. A. Lauffenburger, and P. K. Sorger, *Comparing signaling networks between normal and transformed hepatocytes using discrete logical models*, Cancer Res., 71 (2011), pp. 5400–5411.
[35] J. Saez-Rodriguez, L. Simeoni, J. A. Lindquist, R. Hemenway, U. Bommhardt, B. Arndt, U.-U. Haus, R. Weismantel, E. D. Gilles, S. Klamt, and B. Schraven, *A logical model provides insights into T cell receptor signalling*, PLoS Comput. Biol., 3 (2007), pp. 1580–1590.
[36] R. Schlatter, K. Schmich, I. A. Vizcarra, P. Scheurich, T. Sauter, C. Borner, M. Ederer, I. Merfort, and O. Sawodny, *ON/OFF and beyond—A Boolean model of apoptosis*, PLoS Comput. Biol., 5 (2009), e1000595.
[37] B. Stigler, *Polynomial dynamical systems in systems biology*, in Modeling and Simulation of Biological Networks, Proc. Sympos. Appl. Math. 64, AMS, Providence, RI, 2007, pp. 53–84.
[38] B. Sturmfels, *Gröbner Bases and Convex Polytopes*, AMS, Providence, RI, 1996.
[39] R. Thomas, *Boolean formalization of genetic control circuits*, J. Theoret. Biol., 42 (1973), pp. 563–585.
[40] A. Wuensche, *Complex and chaotic dynamics, basins of attraction, and memory in discrete networks*, Acta Phys. Polon. B, 3 (2010), pp. 463–478.
[41] R. Zhang, M. V. Shah, J. Yang, S. B. Nyland, X. Liu, J. Yun, R. Albert, and T. P. Loughran, *Network model of survival signaling in large granular lymphocyte leukemia*, Proc. Natl. Acad. Sci. USA, 105 (2008), pp. 16308–16313.